Density dependence in group dynamics of a highly social mongoose, Suricata suricatta

Bateman, Andrew W ; Ozgul, Arpat ; Coulson, Tim ; Clutton-Brock, Tim H

Abstract: 1. For social species, the link between individual behaviour and population dynamics is mediated by group-level demography. 2. Populations of obligate cooperative breeders are structured into social groups, which may be subject to inverse density dependence (Allee effects) that result from a dependence on conspecific helpers, but evidence for population-wide Allee effects is rare. 3. We use field data from a long-term study of cooperative meerkats (Suricata suricatta; Schreber, 1776) -a species for which local Allee effects are not reflected in population-level dynamics - to empirically model interannual group dynamics. 4. Using phenomenological population models, modified to incorporate environmental conditions and potential Allee effects, we first investigate overall patterns of group dynamics and find support only for conventional density dependence that increases after years of low rainfall. 5. To explain the observed patterns, we examine specific demographic rates and assess their contributions to overall group dynamics. Although per-capita meerkat mortality is subject to a component Allee effect, it contributes relatively little to observed variation in group dynamics, and other (conventionally density dependent) demographic rates - especially emigration - govern group dynamics. 6. Our findings highlight the need to consider demographic processes and density dependence in subpopulations before drawing conclusions about how behaviour affects population processes in socially complex systems.

DOI: https://doi.org/10.1111/j.1365-2656.2011.01934.x

Density dependence in group dynamics of a highly social mongoose, *Suricata suricatta*

Running Headline: Group dynamics in a highly social species

A. W. Bateman[1,*], A. Ozgul[1], T. Coulson[2], T. H. Clutton-Brock[1]

*corresponding author: awb42@cam.ac.uk

[1]Department of Zoology, University of Cambridge, Downing Street, Cambridge CB2 3EJ United Kingdom

[2]Department of Life Sciences, Imperial College London, Silwood Park, Ascot, Berkshire SL5 7PY United Kingdom

Abstract

1. For social species, the link between individual behaviour and population dynamics is mediated by group-level demography.
2. Populations of obligate cooperative breeders are structured into social groups, which may be subject to inverse density dependence (Allee effects) that result from a dependence on conspecific helpers, but evidence for population-wide Allee effects is rare.
3. We use field data from a long-term study of cooperative meerkats (*Suricata suricatta*) – a species where local Allee effects are not reflected in population-level dynamics – to empirically model inter-annual group dynamics.
4. Using phenomenological population models, modified to incorporate environmental conditions and potential Allee effects, we first investigate overall patterns of group dynamics and only find support for conventional density dependence that increases after years of low rainfall.
5. In order to explain the observed patterns, we examine specific demographic rates and assess their contributions to overall group dynamics. Although we find that per-capita meerkat mortality is subject to an Allee effect, it contributes relatively little to observed variation in group dynamics, and other (conventionally density dependent) demographic rates – especially emigration – govern group dynamics.
6. Our findings highlight the need to consider demographic processes and density dependence in sub-populations before drawing conclusions about how behaviour affects population processes in socially complex systems.

Key Words: Beverton-Holt model, demographic decomposition, environmental effects, Ricker model

Introduction

Across species, populations are often subdivided into smaller units, such as social groups, among which local dynamics interact and combine to produce population-wide patterns. Regardless of the level of organisation, observed dynamics are a consequence of local birth, death, immigration, and emigration processes. To understand a population's dynamics, we therefore need to understand the dynamics of its sub-units and the demographic components that contribute to those dynamics (Coulson *et al.* 2001; Ozgul *et al.* 2009).

For populations of group-living species, social structure likely has important demographic consequences, and can lead to dynamics that are qualitatively different from those of homogeneous populations. In Serengeti lions (*Panthera leo*), for example, periods of population equilibrium were punctuated by periods of abrupt increase while environmental conditions improved gradually (Packer *et al.* 2005), and models that ignore lions' social structure fail to reproduce the observed population dynamics. This is likely true for other highly social species.

Obligate cooperative breeders – species characterised by the presence of non-breeding individuals that help to raise offspring in social groups – are notable in this context for two reasons. First, they present good opportunities to study the relationships among demography, group-level dynamics, and population-level dynamics. Second, they can be subject to Allee effects (positive, or inverse, density dependence in individual demographic rates or per-capita growth rates; Clutton-Brock *et al.* 1999a; Courchamp, Grenfell & Clutton-Brock 1999) acting at the group level but potentially inconspicuous at the population level (Bateman, Coulson & Clutton-Brock 2011). While Allee effects have been widely studied before, the full implications of such effects in obligate

cooperators are unclear, and empirical investigation would contribute to what has been a largely theoretical discussion.

Allee effects can act at two levels. Initially, increasing group or population size may positively affect one or more components of individual fitness, such as the probabilities of survival or successfully raising offspring; Stephens, Sutherland, and Freckleton (1999) define such relationships as "component" Allee effects. These component effects may or may not combine to produce overall "demographic" Allee effects at the group or population level (Stephens, Sutherland & Freckleton 1999). Overall population- or group-level Allee effects (we avoid the term "demographic" Allee effect to avoid confusion when discussing component demographic rates) are most often measured as negative per-capita growth rates of the appropriate unit (Courchamp, Berec & Gascoigne 2008). As one of the potential proximate causes of population decline, these effects are of ultimate relevance for conservation and management and are more easily monitored than component-level effects. To understand when and how component-level effects may translate into population-level effects, we need to investigate the link between the two levels.

Allee effects of one form or another may be common in obligate cooperators (Courchamp, Clutton-Brock & Grenfell 1999), because when group members work together (*e.g.* in hunting, thermoregulation, or alloparental care) they can initially overcome conventional negative density dependence (Allee 1931). The downside for some species may be negative per-capita growth rates in small groups due to their reliance on conspecific helpers, leading to increased risks of group extinction (Courchamp, Grenfell & Clutton-Brock 1999). We might thus expect some signature of Allee effects at the population or group level, but current empirical evidence in obligate

cooperators is sparse and somewhat ambiguous. In African wild dogs (*Lycaon pictus*) there is evidence for Allee effects in specific demographic rates (Courchamp, Grenfell & Clutton-Brock 1999; Courchamp & Macdonald 2001), but recent empirical studies offer limited support and no evidence for group- or population-level effects (Somers *et al.* 2008; Gusset & Macdonald 2010; Woodroffe 2011). In meerkats (*Suricata suricatta*) there is evidence of an Allee effect in survival and circumstantial evidence of an Allee effect in overall group dynamics (Clutton-Brock *et al.* 1999a), but it is unlikely that all demographic rates are affected (Stephens *et al.* 2005), and the only empirical study of meerkats' population-level dynamics found no evidence for an Allee effect (Bateman, Coulson & Clutton-Brock 2011). According to theory, Allee effects in individual demographic rates should not necessarily generate population- or group-level effects, and Allee effects in sub-populations should not necessarily scale up to populations overall (Frank & Brickman 2000), but further empirical work is required to identify the level at which Allee effects break down in populations of obligate cooperators.

A starting point in understanding the population dynamics of obligate cooperators is to understand their group dynamics. We propose a combination of simple group dynamics models and models of constituent demographic rates to link patterns of life history and behaviour with patterns of group dynamics. Phenomenological discrete-time models provide a well-supported basis to describe the dynamics of populations and sub-populations (Brännström & Sumpter 2005; Coulson *et al.* 2008), but they do not account for contributions from underlying demographic rates. To investigate contributions to group dynamics from birth, death, and dispersal, we can combine simple descriptive models that capture density or environmental dependence in each rate (Coulson *et al.* 2008). Assessing contributions from each rate under different conditions can illuminate

how various factors affect group dynamics and may provide clues as to how Allee effects shape the dynamics of obligate cooperators.

Here, we report an empirical investigation of group dynamics in meerkats. Past work has focused on meerkat population-level dynamics, and discussions of Allee effects in cooperative breeders have paid special attention to group-level processes. We therefore chose to focus on group-level dynamics to bridge the gap between behavioural and population-dynamics work. Because they are well-studied behaviourally, and individual-based demographic data exist from more than a decade of field-study in a wild population, meerkats provide an excellent opportunity to investigate the dynamics of obligate cooperative breeders. Employing an information-theoretic approach, we use well-established phenomenological discrete-time models to describe group dynamics and then use simpler models to examine contributions from individual demographic rates to group dynamics. We aim to clarify the importance of Allee effects for meerkats, thereby illustrating the importance of considering the appropriate scale in population dynamics studies more broadly.

Methods

Study Species

Meerkats – social mongooses that inhabit semi-arid regions of southern Africa – form groups of 3 to 50 individuals at approximate population densities of 7-17 individuals/km^2 (Bateman, Coulson & Clutton-Brock 2011). Within groups, reproduction is largely monopolised by a long-lived, behaviourally dominant pair (Clutton-Brock, Hodge & Flower 2008; Sharp & Clutton-Brock 2010), and subordinate individuals help to care for dependent offspring (Clutton-Brock *et al.* 1999b). Females

produce multiple litters per year, but reproduction peaks in January, at the height of the rainy season, and falls to almost nil in July, at the height of the dry season (Clutton-Brock *et al.* 1999b). Before giving birth, dominant females commonly evict subordinate females, sometimes permanently but often temporarily, in an effort to avoid infanticide (Clutton-Brock *et al.* 1998a). Each year, peaking early in the breeding season, some subordinate males and females disperse to join existing groups or form new groups (Doolan & Macdonald 1996), but female immigration is extremely rare (Stephens *et al.* 2005). Although meerkats are arid-adapted, inter-annual variation in rainfall strongly affects their reproduction, survival, and overall population dynamics (Doolan & Macdonald 1997; Clutton-Brock *et al.* 1999a; Bateman, Coulson & Clutton-Brock 2011).

Data Collection

We used individual-based demographic data from a population of habituated, wild meerkats on and near the Kuruman River Reserve (26°58'S, 21°49'E), an area of ranchland near Van Zylsrus in the Northern Cape province of South Africa. A detailed description of the site and local conditions can be found elsewhere (Russell *et al.* 2002).

During weekly (and often daily) visits to meerkat social groups, researchers collected detailed birth, death, immigration, and emigration records for individually marked meerkats (Clutton-Brock *et al.* 1998a; Clutton-Brock, Hodge & Flower 2008). Following Bateman *et al.* (2011), we generated from these data group censuses of individuals older than two months on July 1st (in the height of the dry season between annual pulses of reproduction; Clutton-Brock *et al.* 1999b) for each year between 1998 and 2008.

We often had complete and accurate death and dispersal information for individual meerkats (emigrants recorded in neighbouring groups, carcasses found, or predation observed). For cases of unknown fate, we used knowledge of meerkat behaviour (Clutton-Brock *et al.* 1998a; Clutton-Brock *et al.* 1998b; Clutton-Brock *et al.* 2002; Stephens *et al.* 2005; Russell *et al.* 2007) to assign disappearances as either apparent emigration or apparent death. We deemed individuals that had shown signs of pre-dispersal (*i.e.* spent time outside the group) in the month before disappearance to have emigrated, disappearances of a dominant individual to be deaths, multiple simultaneous same-sex disappearances to be group emigration, and all other disappearances to be deaths. All further references to death and emigration thus refer to apparent death and apparent emigration, respectively.

To estimate population density, we divided population census counts by estimates of the population's range. During group visits, researchers recorded the GPS coordinates of sleeping burrows, which we used to estimate a 95% utilization distribution from an empirical kernel utilisation distribution (Worton 1989) generated with a bivariate normal kernel and fixed smoothing parameter. Further details of GPS data collection and our estimation of population range can be found elsewhere (Jordan, Cherry & Manser 2007; Bateman, Coulson & Clutton-Brock 2011).

We acquired rainfall data using NASA's GIOVANNI (**G**oddard Earth Sciences Data and Information Services Center **I**nteractive **O**nline **V**isualization **AN**d a**N**alysis **I**nfrastructure) data system (NASA 2009). GIOVANNI provides monthly rainfall estimates based on 2.5^{o} x 2.5^{o} (latitude x longitude) gridded rainfall data from the Global Precipitation Climatology Project Version 2.1 Combined Precipitation Dataset (an update of the version 2 dataset described in Adler *et al.* 2003).

Modeling Approach

We used an information-theoretic approach (Akaike 1973; Burnham & Anderson 2002) to compare models, which represented competing hypotheses, describing meerkat group dynamics and demographic rates. In each instance, we first generated a candidate set of discrete-time models. Next, we used maximum-likelihood techniques to fit each model to annual meerkat group size data, estimating best-fit model parameters in the process (for a detailed description see Hilborn & Mangel 1997 or Bolker 2008). With the resulting negative log-likelihoods, we calculated Akaike's Information Criterion (AIC;Akaike 1973), ΔAIC relative to the minimum AIC model, and Akaike model weights for each model (see Burnham & Anderson 2002 for details). Lower AIC values represent "better" (more parsimonious) models; $\Delta\text{AIC} \leq 2$ indicates a model with substantial support, while $\Delta\text{AIC} \geq 10$ indicates a model with essentially no support; and each Akaike model weight (w) is interpreted as the probability that the associated model is the "best" (most parsimonious) model, given the candidate model set (Burnham & Anderson 2002).

Phenomenological Group Dynamics Models

The core models for our overall analysis of group dynamics were standard discrete-time population dynamics models. We used these to predict group dynamics in year-long intervals, or time steps, between annual group size observations. At their simplest, these models take the form

$$N_{t+1} = N_t \cdot \lambda(N_t)\,, \tag{1}$$

where N_t is group size at the beginning of year t and λ is a density-dependent function defining per-capita group growth rate ($\lambda_t = N_{t+1}/N_t$). Note that t enumerates a model timestep and not a calendar year; each year t spans two calendar years, from July 1st of one to June 30th of the next.

Many possible models exist in the literature, but most fall into two categories describing different types of competition among individuals: contest and scramble (Brännström & Sumpter 2005). In both cases λ declines as N_t increases, but under contest competition a number of individuals, as determined by habitat quality, are always able to secure sufficient resources, and N_{t+1} is an increasing function of N_t, whereas under scramble competition each additional competitor reduces the resources secured by its conspecifics, and N_{t+1} initially increases but then peaks and declines to zero for large N_t. Classic models of contest and scramble competition are the Beverton-Holt (Beverton & Holt 1957) and Ricker (Ricker 1954) models, respectively. The Beverton-Holt model takes the form

$$N_{t+1} = N_t \cdot \frac{\lambda_0}{1 + N_t\left(\frac{\lambda_0 - 1}{K}\right)}, \tag{2}$$

where λ_0 is the theoretical per-capita growth rate at $N_t = 0$, and K is the population (group) carrying capacity. The Ricker model takes the form

$$N_{t+1} = N_t \cdot \lambda_0^{\left(1 - \frac{N_t}{K}\right)}. \tag{3}$$

While refinements to these models and different functional forms might capture other subtleties in dynamics, for our purposes, models (2) and (3) were sufficient to describe relevant patterns.

Incorporating Rainfall and Density

Previous research has shown that rainfall in year t, and possibly in year t-1, affects population dynamics in year t (Bateman, Coulson & Clutton-Brock 2011), and we wanted to consider the possibility that population density (meerkats/km^2 across the study site) affects group-level dynamics. We therefore extended the Beverton-Holt and Ricker models above to incorporate effects of rainfall and population density such that

$$N_{t+1} = N_t \cdot \lambda\left(N_t, R_t, R_{t-1}, D_t\right). \quad (4)$$

To do this, we assumed that λ_0 and K are functions of total rainfall in year t-1 and t ($R_{t\text{-}1}$ and R_t, respectively) and density at the beginning of year t (D_t). As first-order approximations of what may be the "true" nonlinear relationships, we used linear functions:

$$\begin{aligned} \lambda_0 &= a_0 + a_1 D_t + a_2 R_t + a_3 R_{t-1} \text{ and} \\ K &= b_0 + b_1 D_t + b_2 R_t + b_3 R_{t-1} \end{aligned} \quad (5)$$

within the phenomenological models, considering a set of models that included different combinations of the individual effects of R_t, $R_{t\text{-}1}$, and D_t (see next section for incorporation of Allee effects). Models that included $R_{t\text{-}1}$ also included R_t for biological realism. For model fitting, we centred (subtracted the sample mean value) and normalized (divided by the sample standard deviation) annual rainfall measures. Our initial set included twelve group dynamics models, six variants for each of the Beverton-Holt and Ricker basic forms (Table 1).

Making the assumption that errors were negative binomially distributed, we fit each candidate model to our set of group time series, estimating one set of parameters across all groups in the study population. Given the nature of our data collection regime, observation error is negligible, and we assumed that group dynamics were subject to

process error only (Hilborn & Mangel 1997). In practice, this meant that the likelihood we calculated for each group size observation, given a model, came from a negative binomial distribution with mean predicted by the model (incorporating the group's size in the previous year as well as the appropriate rainfall and population density information) and shape parameter fit as an additional free parameter.

Allee Effects in Group Dynamics

After fitting the initial candidate models, we assessed the presence of a group-level Allee effect, taking as a starting point the group dynamics models from the initial candidate set with greater than 10% support based on Akaike model weights. We modified the form of the per-capita growth rate in these models by raising $\lambda(N_t,R_t,R_{t-1},D_t)$ to an Allee exponent term:

$$N_{t+1} = N_t \cdot \lambda_{\text{mod}} = N_t \cdot \lambda\left(N_t, R_t, R_{t-1}, D_t\right)^{\left(\frac{N_t - d}{N_t}\right)}. \quad (6)$$

This modification represents a strong Allee effect, where d is the (positive) Allee parameter, or threshold, indicating the group size below which group size declines in year t. K remains unchanged (since $\lambda = 1$ at K, and $1^a = 1$ for all a), but λ_0 no longer represents initial per-capita growth rate, but rather the theoretical initial per-capita growth rate in the absence of an Allee effect.

Although strong Allee effects are a specific sub-class of Allee effects in general, they do not have special properties above their Allee threshold, and more general models use an additional degree of freedom. Given that our data were sparse at low initial group sizes (Figure 2), our ability to distinguish between strong and weak Allee effects was minimal, so we considered only the modification in (6).

Adopting the approach of Bolker (2008) to estimate confidence intervals for parameters on the edge of their allowable ranges, we used the likelihood surface approach to calculate 95% confidence intervals for d in each modified model to assess precision of the estimated Allee effects.

Demographic Rates

To explain the results of phenomenological modelling, we decomposed group dynamics into contributions from constituent demographic rates. For any social group (and indeed for any unit of population generally) changes in group size must obey

$$N_{t+1} = N_t + B_t - M_t + I_t - E_t, \tag{7}$$

where B_t, M_t, I_t, and E_t enumerate recruitment (here at two months of age), mortality, immigration, and emigration, respectively, in year t. Rearranging (7), we can write

$$N_{t+1} = N_t + B_t + I_t - \left(N_t + B_t + I_t\right)\left(\frac{E_t + M_t}{N_t + B_t + I_t}\right)$$

$$= \left(N_t + B_t + I_t\right)\left(1 - \frac{E_t}{N_t + B_t + I_t} - \frac{M_t}{N_t + B_t + I_t}\right)$$

$$= N_t\left(1 + \bar{B}_t + \bar{I}_t\right)\left(1 - \bar{E}_t - \bar{M}_t\right), \tag{8}$$

where $\bar{B}_t$, $\bar{M}_t$, $\bar{I}_t$, and $\bar{E}_t$ are the per-capita versions of B_t, M_t, I_t, and E_t, respectively. Note that (8) makes the implicit assumption that mortality and emigration are preceded by recruitment and immigration and that the rates of influx, $\bar{B}_t$ and $\bar{I}_t$, are relative to initial group size (N_t) and are bounded below by zero, while the rates of efflux, $\bar{M}_t$ and $\bar{E}_t$, are relative to the total number of individuals present in the associated group at some point in year t ($N_t+B_t+I_t$) and lie between zero and one (inclusive).

The different properties of each influx and efflux rate, as described above, necessitated different modeling approaches. We used a linear function of N_t, R_t, and $R_{t\text{-}1}$ (the model terms from the most parsimonious group-dynamics model – see results section), plus interactions, to predict each log-transformed mean per-capita rate of influx, $\overline{r}_{influx\ i,t}$, so that

$$\overline{r}_{influx\ i,t} = e^{\left(c_0 + c_1 N_t + c_2 R_t + \ldots\right)}. \tag{9}$$

Because B_t and I_t take integer values, we fit models to observed values of these influx rates, $r_{influx\ i,t}$, assuming negative binomial error distributions:

$$r_{influx\ i,t} \sim \text{negative binomial}\left(\mu = N_t \cdot \overline{r}_{influx\ i,t}, \eta\right), \tag{10}$$

where η is the negative binomial shape parameter, which we fit as a free parameter for each rate. We assumed that each logit-transformed mean per-capita rate of efflux was a linear function of N_t, R_t, $R_{t\text{-}1}$, plus interactions, so that

$$\overline{r}_{efflux\ i,t} = \left(1 + e^{-\left(c_0 + c_1 N_t + c_2 R_t + \ldots\right)}\right)^{-1}. \tag{11}$$

For an individual, present in a given group in year t, (11) represents the probability of death or the probability of emigration by the start of year t+1. We modeled observed values of M_t and E_t assuming a binomial distribution:

$$r_{efflux\ i,t} \sim \text{binomial}\left(p = \overline{r}_{efflux\ i,t}, n = N_t + B_t + I_t\right). \tag{12}$$

While we did not include interaction terms in the linear functions for λ_0 and K in the group dynamics models, λ_0 is the initial value and K controls the steepness of the per-capita group growth rate in those models. By including interaction terms in the per-capita demographic rate models, we allowed the predictor variables to have potentially similar control over each predicted demographic rate.

Our candidate model set for the demographic rates consisted of the models described above with distinct c_i coefficients for each rate (Table 2). We found the most parsimonious model for each rate independently and then combined those models to generate predictions of N_{t+1} as follows.

Let $\theta_t = \{N_t,\ R_t,\ R_{t-1}\}$, the set of conditions in year t. Using $\mathrm{P}(B_t = x \mid \theta_t)$ and $\mathrm{P}(I_t = x \mid \theta_t)$, given by (9) and (10), the distribution for total influx, ($\Phi_t = B_t + I_t$), becomes

$$\mathrm{P}(\Phi_t = x \mid \theta_t) = \sum_{j=0}^{\infty} \mathrm{P}(B_t = j \mid \theta_t) \cdot \mathrm{P}(I_t = x - j \mid \theta_t)\,. \qquad (13)$$

Now, $\bar{M}_t$ and $\bar{E}_t$, given by (11), are the probabilities of mortality and emigration, respectively, for an individual present in a given group in year t. $\bar{S}_t = 1 - \bar{M}_t - \bar{E}_t$ is, therefore, the probability that an individual present in year t is present at the start of year t+1. The conditional group size distribution for year t+1 becomes

$$\mathrm{P}(N_{t+1} = x \mid \theta_t, \Phi_t) = \mathrm{P}_{binomial}(p = \bar{S}_t,\ n = N_t + \Phi_t)\,. \qquad (14)$$

Summing over all possible values of Φ_t, we get the unconditional distribution for N_{t+1}:

$$\mathrm{P}(N_{t+1} = x \mid \theta_t) = \sum_{j=0}^{\infty} \mathrm{P}(\Phi_t = j \mid \theta_t) \cdot \mathrm{P}(N_{t+1} = x \mid \theta_t, \Phi_t = j)\,, \qquad (15)$$

from which we calculated the expected values of N_{t+1}:

$$\mu(N_{t+1})\big|_{\theta_t} = \sum_{x=0}^{\infty} \left[x \cdot P(N_{t+1} = x \mid \theta_t) \right] = \sum_{x=0}^{\infty} \left[x \cdot \sum_{j=0}^{\infty} \mathrm{P}(\Phi_t = j \mid \theta_t) \cdot \mathrm{P}(N_{t+1} = x \mid \theta_t, \Phi_t = j) \right]$$

$$= \sum_{j=0}^{\infty} \left[\mathrm{P}(\Phi_t = j \mid \theta_t) \cdot \sum_{x=0}^{N_t + j} x \cdot \mathrm{P}(N_{t+1} = x \mid \theta_t, \Phi_t = j) \right]$$

$$= \sum_{j=0}^{\infty} \mathrm{P}(\Phi_t = j \mid \theta_t) \cdot (\bar{S}_t) \cdot (N_t + j)\,, \qquad (16)$$

using the fact that the expected value of a binomial random variable with parameters n and p is n·p.

Assessing Model Contributions

To estimate the explanatory power of the most parsimonious models, as selected by AIC, and of different model components, we used R^2, which gives the proportion of total variation in data explained by a model fit to those data. As a measure of goodness of fit, standard R^2 has its limitations, but it provides a reasonable sense of how well a model describes data (Kvålseth 1985).

Because a random walk is the appropriate null model for population dynamics with pure process error, we would not expect each group's size to fluctuate about some mean value, but rather about $N_t \cdot \lambda$, where λ is a constant value (typically one, not dependent on θ_t) for all t. We used $\hat{\lambda}$, the maximum-likelihood constant estimate for $\lambda(N_t)$ in (1), to estimate λ and calculated R^2 based on predicted and observed group sizes, taking total sum of squares to be $\sum_{\text{all groups, } t} (N_{t+1} - N_t \cdot \hat{\lambda})^2$.

We also used R^2 to assess the explanatory power of different model components. The difference between the R^2 value of a maximally parsimonious model and the R^2 value of the same model without a component of interest gives an estimate of that component's contribution to the model fit (Coulson *et al.* 2008). We assessed the contributions of R_t, R_{t-1}, and density dependence in λ_t (by using the mean value of N_t in estimation of λ_t) for the phenomenological dynamics models, and we assessed the contributions of R_t, R_{t-1}, and N_t overall and through their contributions to individual demographic rates, as well as the contribution from each demographic rate model (by

fixing the predicted rate at its observed mean), in the combined model of demographic rates in (15).

Statistical Software

We carried out analyses in R (R Development Core Team 2011). To minimize model negative log-likelihoods, we used the *optim* optimizer for models of demographic rates and the *genoud* optimizer from the *rgenoud* package for group dynamics models (*genoud* combines *optim*'s quasi-Newton optimization algorithm with a genetic optimization algorithm in an effort to avoid "getting stuck" at local optima; Mebane Jr & Sekhon 2011). For kernel home range estimation we used the *kernelUD* function in the *adehabitat* package (Calenge 2006).

Results

Data

We recorded a total of 104 group-years over the ten years of the study. Group sizes on July 1st ranged from 4 to 47 individuals, with a mean of 17.7; population density on July 1st ranged from 7.5 to 17.1 individuals per km^2, with a mean of 11.7; and annual rainfall ranged from 178.6 to 473.4 mm, with a mean of 294.4.

Phenomenological Models

The best models from our candidate set were those that incorporated both annual rainfall in year *t* and annual rainfall in year *t*-1. Overall, the Ricker model of this form was the most parsimonious, but the corresponding Beverton-Holt model had a ΔAIC of

less than two. Together, these models shared more than 85% of model support, while no other model had more than 10% support (Table 1).

The parameter estimates in the best Ricker model gave $\lambda_0 = 1.45 + 0.16 \cdot R_t - 0.21 \cdot R_{t-1}$, and $K = 27.34 - 0.62 \cdot R_t + 14.06 \cdot R_{t-1}$, with a negative binomial shape parameter of 15.71. The parameter estimates in the best Beverton-Holt model gave $\lambda_0 = 1.72 + 0.23 \cdot R_t - 0.34 \cdot R_{t-1}$, and $K = 24.47 - 0.20 \cdot R_t + 12.32 \cdot R_{t-1}$, with a negative binomial shape parameter of 15.02. This meant that in both best models the main effects of rainfall were those associated with R_{t-1}; the best models both describe group dynamics in which per-capita group growth rates decline in large groups after years of low rainfall (Figure 1).

Allee Effects

We fit Allee effect-modified versions of the best-fitting Ricker and Beverton-Holt models (which we refer to as "Allee-Ricker" and "Allee-Beverton-Holt" models, respectively). In both cases, the maximum-likelihood Allee parameter estimates were zero, reproducing the dynamics of the non-Allee effect parent model forms. AIC values for the Allee models were simply two units higher due to one additional parameter but the same negative log-likelihood as their non-Allee counterparts.

95% confidence intervals for the Allee parameters were [0, 4.3] for the Allee-Ricker model and [0, 4.0] for the Allee-Beverton-Holt model. Comparing the maximum-likelihood fit of the Allee-Ricker model with Allee parameter 4.3 to the maximum-likelihood fit overall (Figure 2), we see that the two models give almost identical predictions across the range of observed group sizes and that very few observations exist for small groups which might arbitrate between the two model forms.

Demographic Rates

Different per-capita rates were best predicted by different combinations of variables (Table 2). Of the models considered, the most parsimonious model for mean per-capita recruitment was $N_t \cdot \exp(-0.11 - 0.04 \cdot N_t + 0.1 \cdot R_t)$, with a negative binomial shape parameter of 5.52; the most parsimonious model for mean per-capita immigration was $N_t \cdot \exp(-0.19 - 0.03 \cdot N_t)$, with a negative binomial shape parameter of 0.16; the most parsimonious model for per-capita mortality rate was $[1+\exp(1.39 + 0.03 \cdot N_t - 0.76 \cdot R_{t-1} - 0.22 \cdot R_t + 0.03 \cdot N_t \cdot R_{t-1} + 0.02 \cdot N_t \cdot R_t)]^{-1}$; and the most parsimonious model for per-capita emigration rate was $[1+\exp(1.83 - 0.03 \cdot N_t + 0.10 \cdot R_{t-1} + 0.01 \cdot N_t \cdot R_{t-1})]^{-1}$.

Annual per-capita recruitment declined with increasing initial group size and increased with annual rainfall (Figure 3A). Per-capita immigration declined with increasing initial group size (Figure 3B). Per-capita mortality tended to decline with increasing initial group size (the only rate-specific Allee effect), with the trend more pronounced after years of high rainfall (Figure 3C). Per-capita emigration increased with increasing initial group size and was lower, especially in large groups, after years of high rainfall (Figure 3D).

Combining all the demographic rates together into a "combined demographic" model yielded group dynamics predictions (Figure 4) similar to those from the best phenomenological models. While the effect of past rainfall was not as strong as in the phenomenological models, it was still clearly present.

The combined demographic model, unlike the best-fitting phenomenological models, can describe a group-level Allee effect if Allee effects of sufficient magnitude exist in individual demographic rates. In two years, 2000 and 2006, the Allee effect

present in the mortality model was strong enough to produce an overall group-level Allee effect in the combined demographic model (Figure 5).

Model Contributions

The best group dynamics models explained between 32% and 39% of the observed variation in group size, with the Ricker model explaining the most variation (Table 3). In all three models (Ricker, Beverton-Holt, and combined demographic), rainfall in year t-1 was responsible for far more of the explanatory power than rainfall in year t (43-49% compared with 2-7%, respectively). Within the component demographic model, the sub-model describing per-capita emigration explained more variation than did any other per-capita rate model. The majority of the explanatory power of the emigration model resulted from the inclusion of $R_{t\text{-}1}$ terms, and inclusion of $R_{t\text{-}1}$ in the emigration model accounted for the majority of the explanatory power of $R_{t\text{-}1}$ in the combined demographic model overall.

Discussion

We investigated the relationship between demographic processes and group dynamics in meerkats, obligate cooperative breeders for which group dynamics have been assumed to exhibit Allee affects. Although we found a component Allee effect in rates of mortality, all other demographic rates were conventionally density dependent. Combination of component rate models successfully reproduced group dynamics, as described by phenomenological models. Mortality rates contributed relatively little to group dynamics, however, and the associated component Allee effect failed to produce an overall (demographic) Allee effect at the group level.

Overall Group Dynamics

Using field data from a long-term study, we compared competing models of inter-annual meerkat group-size dynamics, assessing support for models describing contest and scramble competition, effects of rainfall and population density, and a group-level Allee effect. Because neither the Ricker nor the Beverton-Holt model form was clearly better at describing group dynamics, we were unable to distinguish between contest and scramble competition. We found good support for effects of two years' past rainfall but little support for an effect of population density. The best model explained almost 40% of the observed variation in group size but did not include an Allee effect. Observations for groups smaller than five individuals were limited (Figure 2), and uncertainty in the Allee parameters reflected this. Still, the most parsimonious descriptions of meerkat group dynamics within the range of observations, and even the best-fitting Allee effect models themselves, did not include an Allee effect. Instead, conventional density dependence was evident and increased after years of relatively low rainfall (Figure 1), an effect that accounted for nearly half of the best model's ability to explain group dynamics (Table 3).

The lack of an obvious Allee effect, and stronger conventional density dependence after low-rainfall years, is somewhat surprising, given that past studies have suggested that meerkats derive considerable benefits from living in larger groups (Clutton-Brock *et al.* 2001; Hodge *et al.* 2008) and that small groups suffer disproportionate negative effects in bad years (Clutton-Brock *et al.* 1999a). There are two potential explanations for this inability to detect an Allee effect: we may have missed

an Allee effect present in small groups, or Allee effects in component demographic rates may not translate to the group level.

Constituent Demography

To assess contributions to group dynamics from different demographic components, we constructed a group dynamics model from models of individual demographic rates. First, we used simple models to describe the effects of rainfall and group size on recruitment, immigration, mortality, and emigration. Next, we assembled the models of individual rates into a combined demographic model of group dynamics. The resulting model predictions matched those of our earlier phenomenological models well (Figures 1, 4) and explained a similar amount of variation (Table 3), lending support to our subsequent assessment of each model term's explanatory power.

Our treatment of individual demographic rates illuminates the observed patterns of group dynamics. As previously described (Clutton-Brock *et al.* 1999a), meerkat mortality tends to decrease with increasing group size (Figure 3C). Recruitment, immigration, and emigration, however, are conventionally density dependent (Figures 3A,B,D). Emigration accounted for the largest proportion of variation explained by the combined demographic model. Mortality – the only demographic rate subject to an Allee effect – accounted for relatively little (Table 3). This explains why overall group dynamics, as described by the best phenomenological models, did not exhibit an Allee effect.

The combined demographic model did exhibit a demographic Allee effect in two out of ten years, but this is likely a case of overfitting: the combined demographic model has more parameters and actually exhibits a poorer fit to the data than the best

phenomenological models (Table 3), and the apparent Allee effect is not well-supported by the data (Figure 5).

Interpretation

The existence of inverse density dependence in meerkat mortality rates – the feature of meerkat biology that initially sparked interest in potential Allee effects (Clutton-Brock *et al.* 1999a) – has at least two possible interpretations. First, meerkat sentinel behaviour may help individuals in larger groups to avoid predation, and second, small groups may suffer from an inability to compete for hospitable territories (Clutton-Brock *et al.* 1999a). Because reduced mortality in small groups after years of low rainfall coincides with reductions in population density (Bateman, Coulson & Clutton-Brock 2011), which likely reduces intergroup competition, our results offer support for the latter.

Conventional density dependence in recruitment seems at first paradoxical, since dominant female reproductive output, which constitutes the majority of reproductive success for any group (Clutton-Brock *et al.* 1999b; Clutton-Brock, Hodge & Flower 2008), increases with group size (Hodge *et al.* 2008). The simple explanation is that recruitment increases do not keep pace with increasing group size, leading to reduced per-capita recruitment in larger groups (Figure 3A). A similar result is likely to explain patterns observed in wild dogs, in which breeding females produce more offspring in larger groups but population dynamics show conventional density dependence (Woodroffe 2011).

Dispersal patterns are consistent with a pattern of dominant control over female group membership and almost exclusive male immigration. Subordinate females

jeopardize dominant reproductive success through infanticide (Young & Clutton-Brock 2006; Hodge *et al.* 2008), which dominants avoid by evicting potential same sex rivals (Stephens *et al.* 2005; Young *et al.* 2006), leading to increased eviction rates in larger groups (Clutton-Brock, Hodge & Flower 2008). There is some indication that dominant reproductive output levels-off at group sizes of 20 to 25 (Hodge *et al.* 2008) – the approximate stable group size (Figures 1, 4) – and female emigration is predicted to be under dominant control over most of the range of group size we observed (Stephens *et al.* 2005). Taken together, these suggest that dominant females use eviction to regulate group size in order to maximize their own reproductive success. Males, on the other hand, tend to emigrate of their own accord, but we would also expect male emigration to increase with group size, since larger groups can produce larger, more successful multi-male "coalitions" (Young, Spong & Clutton-Brock 2007) to seize dominance at neighbouring, typically small (Figure 3B) groups.

Dispersal processes have the ability to affect population dynamics beyond their direct contributions to group dynamics. Dispersers may join existing groups, form their own groups, or die before joining new groups. Over large spatial scales, the surrounding population may be heterogeneous, with group formation and augmentation rates varying accordingly. The average emigration rates that we observe are substantially higher than those of immigration (Figure 3). Combined with the fact that patterns of local population density closely correspond to group size dynamics (Bateman, Coulson & Clutton-Brock 2011, Bateman *et al.* in prep.) this suggests that group formation and extinction have reached an equilibrium, locally at least, and dispersers either die or leave the area. More work will be required to elucidate further consequences of dispersal.

The importance of rainfall in meerkat group dynamics is not surprising, but our results help clarify the effects. A number of studies have shown the positive effect of rainfall on breading success (Doolan & Macdonald 1997; Clutton-Brock *et al.* 1999b; Hodge *et al.* 2008), likely mediated by rain's effect on food availability (Doolan & Macdonald 1997) and physical condition (English, Bateman & Clutton-Brock in press) and physical condition's effect on reproductive success (Doolan & Macdonald 1997; Hodge *et al.* 2008). The increase in apparent emigration after years of low rainfall (Figure 3D) is, however, the single aspect of demography with the largest effect on group dynamics (Table 3). This increase may be due to increased extra-group mortality rates that result from reduced physical condition in temporary female evictees and male prospectors. Alternatively, changes to group age structure may play a more important role. In a year of low rainfall, reproduction is limited (Figure 3A), increasing the proportion of subordinates above one year of age in the subsequent year. Because older subordinates are more likely to disperse and suffer eviction (Clutton-Brock *et al.* 2002; Clutton-Brock, Hodge & Flower 2008), such an effect could result in an increase in emigration rates after dry years. More detailed, age-specific analyses will be required to differentiate between these two scenarios.

Conclusions

In addition to the birth and death processes that regulate any population, group size in social species is regulated by immigration and emigration decisions on the part of individuals. The factors affecting these decisions vary: dominant female meerkats may control group sizes through eviction of subordinates at a cost to subordinate fitness (Stephens *et al.* 2005), while female lions remain in prides of a size that maximizes

territory defensibility and reproductive success at the cost of foraging success (Clutton-Brock *et al.* 2000; Mosser & Packer 2009; VanderWaal, Mosser & Packer 2009). Regardless, these behavioural decisions combine with birth and death processes to produce a stable group size and can lead to density dependence in groups similar to that observed in many non-social populations. Classic phenomenological population models, designed with birth and death in mind, were thus able to describe average meerkat group dynamics.

Our results modify our view of meerkat group dynamics. Past work has invoked an Allee effect to explain observed patterns of group dynamics, particularly the high rates of group extinction, especially of small groups, in bad years (Clutton-Brock *et al.* 1999b; Courchamp, Grenfell & Clutton-Brock 1999). As previously noted (Clutton-Brock *et al.* 1999b), group growth rates are low (group size predictions are never far from the 1:1 lines in Figures 1 and 4), but the conventional density dependence we describe here likely explains past results. Given the stochastic nature of group dynamics and meerkats' susceptibility to environmental fluctuations, we would expect small groups to be prone to extinction, even if changes in mean group size are conventionally density dependent.

We have highlighted the importance of sub-population processes and the idea that those processes can display conflicting patterns, leading to non-intuitive dynamics. Allee effects may represent a case study for such dynamical complexity across species. Past evidence for an Allee effect in one aspect of meerkat demography lead to the assumption that group dynamics were inversely density dependent, but this now seems inaccurate. Given that meerkat group-level dynamics appear conventionally density dependent, it is unsurprising that an Allee effect has not been found in meerkat population-level dynamics (Bateman, Coulson & Clutton-Brock 2011). Although Allee effects have broad

theoretical support (Courchamp, Berec & Gascoigne 2008) and have been sought across taxa, there are relatively few convincing population-wide examples (Myers *et al.* 1995; Gregory *et al.* 2010). In such a situation, with obvious implications for conservation and management decisions, it would be prudent to consider population dynamics in the context of population structure (Frank & Brickman 2000) and demographic sub-processes before drawing firm conclusions.

Our analysis of meerkat demography suggests that different drivers affect different demographic rates, but we ignored inter-individual variation in those rates. Because meerkats live in groups made up of multiple age and dominance classes, demographic rates (such as dispersal) differ among classes, and different drivers within each class could increase the impact of this class structure on dynamics (Coulson *et al.* 2008), future work will focus on incorporating class structure into our models.

Acknowledgements

Our thanks go to the tireless staff and volunteers of the Kalahari Meerkat Project, without whom this work would have been impossible, and to R Mares and S Sharp for helpful comments on previous versions of this manuscript. AB would like to thank NSERC Canada and the Cambridge Overseas and Commonwealth trusts and Department of Zoology for funding to carry out this research.

References

Adler, R.F., Huffman, G.J., Chang, A., Ferraro, R., Xie, P.P., Janowiak, J., Rudolf, B., Schneider, U., Curtis, S. & Bolvin, D. (2003) The version-2 global precipitation climatology project (GPCP) monthly precipitation analysis (1979–present). *Journal of Hydrometeorology,* **4,** 1147-1167.

Akaike, H. (1973) Information theory and an extension of the maximum likelihood principle. *Second International Symposium on Information Theory* (eds P.B. N. & C. F.), pp. 268–281. Akadémiai Kiadó, Budapest.

Allee, W.C. (1931) Co-Operation Among Animals. *American Journal of Sociology,* **37,** 386.

Bateman, A.W., Coulson, T. & Clutton-Brock, T.H. (2011) What do simple models reveal about the population dynamics of a cooperatively breeding species? *Oikos,* **120,** 787-794.

Beverton, R.J.H. & Holt, S.J. (1957) On the dynamics of exploited fish populations. *UK Ministry of Agriculture, Fisheries and Food. Investigations (Ser. 2),* **19,** 533.

Bolker, B.M. (2008) *Ecological models and data in R*. Princeton Univ. Press.

Brännström, Å. & Sumpter, D.J.T. (2005) The role of competition and clustering in population dynamics. *Proceedings of the Royal Society of London Series B-Biological Sciences,* **272,** 2065-2072.

Burnham, K.P. & Anderson, D.R. (2002) *Model selection and multimodel inference: a practical information-theoretic approach*. Springer Verlag.

Calenge, C. (2006) The package "adehabitat" for the R software: A tool for the analysis of space and habitat use by animals. *Ecological Modelling,* **197,** 516-519.

Clutton-Brock, T.H., Brotherton, P.N.M., O'Riain, M.J., Griffin, A.S., Gaynor, D., Sharpe, L., Kansky, R., Manser, M.B. & McIlrath, G.M. (2000) Individual contributions to babysitting in a cooperative mongoose, Suricata suricatta. *Proceedings of the Royal Society of London. Series B: Biological Sciences,* **267,** 301-305.

Clutton-Brock, T.H., Brotherton, P.N.M., Smith, R., McIlrath, G.M., Kansky, R., Gaynor, D., O'Riain, M.J. & Skinner, J.D. (1998a) Infanticide and expulsion of females in a cooperative mammal. *Proceedings of the Royal Society of London Series B-Biological Sciences,* **265,** 2291-2295.

Clutton-Brock, T.H., Gaynor, D., Kansky, R., MacColl, A.D.C., McIlrath, G., Chadwick, P., Brotherton, P.N.M., O'Riain, J.M., Manser, M. & Skinner, J.D. (1998b) Costs of cooperative behaviour in suricates (*Suricata suricatta*). *Proceedings of the Royal Society of London Series B-Biological Sciences,* **265,** 185-190.

Clutton-Brock, T.H., Gaynor, D., McIlrath, G.M., Maccoll, A.D.C., Kansky, R., Chadwick, P., Manser, M., Skinner, J.D. & Brotherton, P.N.M. (1999a) Predation, group size and mortality in a cooperative mongoose, *Suricata suricatta*. *Journal of Animal Ecology,* **68,** 672-683.

Clutton-Brock, T.H., Hodge, S.J. & Flower, T.P. (2008) Group size and the suppression of subordinate reproduction in Kalahari meerkats. *Animal Behaviour,* **76,** 689-700.

Clutton-Brock, T.H., Maccoll, A., Chadwick, P., Gaynor, D., Kansky, R. & Skinner, J.D. (1999b) Reproduction and survival of suricates (*Suricata suricatta*) in the southern Kalahari. *African Journal of Ecology,* **37,** 69-80.

Clutton-Brock, T.H., Russell, A.F., Sharpe, L.L., Brotherton, P.N.M., McIlrath, G.M., White, S. & Cameron, E.Z. (2001) Effects of helpers on juvenile development and survival in meerkats. *Science,* **293,** 2446-2449.

Clutton-Brock, T.H., Russell, A.F., Sharpe, L.L., Young, A.J., Balmforth, Z. & McIlrath, G.M. (2002) Evolution and development of sex differences in cooperative behavior in meerkats. *Science,* **297,** 253-256.

Coulson, T., Catchpole, E.A., Albon, S.D., Morgan, B.J.T., Pemberton, J.M., Clutton-Brock, T.H., Crawley, M.J. & Grenfell, B.T. (2001) Age, sex, density, winter weather, and population crashes in Soay sheep. *Science,* **292,** 1528-1531.

Coulson, T., Ezard, T.H.G., Pelletier, F., Tavecchia, G., Stenseth, N.C., Childs, D.Z., Pilkington, J.G., Pemberton, J.M., Kruuk, L.E.B., Clutton-Brock, T.H. & Crawley, M.J. (2008) Estimating the functional form for the density dependence from life history data. *Ecology,* **89,** 1661-1674.

Courchamp, F., Berec, L. & Gascoigne, J. (2008) *Allee effects in ecology and conservation*. Oxford Univ. Press.

Courchamp, F., Clutton-Brock, T. & Grenfell, B. (1999) Inverse density dependence and the Allee effect. *Trends in Ecology & Evolution,* **14,** 405-410.

Courchamp, F., Grenfell, B. & Clutton-Brock, T. (1999) Population dynamics of obligate cooperators. *Proceedings of the Royal Society of London Series B-Biological Sciences,* **266,** 557-563.

Courchamp, F. & Macdonald, D.W. (2001) Crucial importance of pack size in the African wild dog *Lycaon pictus*. *Animal Conservation,* **4,** 169-174.

Doolan, S.P. & Macdonald, D.W. (1996) Dispersal and extra-territorial prospecting by slender-tailed meerkats (*Suricata suricatta*) in the south-western Kalahari. *Journal of Zoology (London),* **240,** 59-73.

Doolan, S.P. & Macdonald, D.W. (1997) Breeding and juvenile survival among slender-tailed meerkats (*Suricata suricatta*) in the south-western Kalahari: Ecological and social influences. *Journal of Zoology (London),* **242,** 309-327.

English, S., Bateman, A. & Clutton-Brock, T. (in press) Lifetime growth in wild meerkats: incorporating life history and environmental factors into a standard growth model. *Oecologia*.

Frank, K.T. & Brickman, D. (2000) Allee effects and compensatory population dynamics within a stock complex. *Canadian Journal of Fisheries and Aquatic Sciences,* **57,** 513-517.

Gregory, S., Bradshaw, C., Brook, B. & Courchamp, F. (2010) Limited evidence for the demographic Allee effect from numerous species across taxa. *Ecology,* **91,** 2151-2161.

Gusset, M. & Macdonald, D.W. (2010) Group size effects in cooperatively breeding African wild dogs. *Animal Behaviour,* **79,** 425-428.

Hilborn, R. & Mangel, M. (1997) *The ecological detective: confronting models with data*. Princeton Univ Pr.

Hodge, S.J., Manica, A., Flower, T.P. & Clutton-Brock, T.H. (2008) Determinants of reproductive success in dominant female meerkats. *Journal of Animal Ecology,* **77,** 92-102.

Jordan, N.R., Cherry, M.I. & Manser, M.B. (2007) Latrine distribution and patterns of use by wild meerkats: implications for territory and mate defence. *Animal Behaviour,* **73,** 613-622.

Kvålseth, T.O. (1985) Cautionary note about R 2. *American Statistician,* **39,** 279-285.
Mebane Jr, W.R. & Sekhon, J.S. (2011) Genetic Optimization Using Derivatives: The rgenoud Package for R. *Journal of Statistical Software,* **42**.
Mosser, A. & Packer, C. (2009) Group territoriality and the benefits of sociality in the African lion, *Panthera leo*. *Animal Behaviour,* **78,** 359-370.
Myers, R.A., Barrowman, N.J., Hutchings, J.A. & Rosenberg, A.A. (1995) Population-dynamics of exploited fish stocks at low population-levels. *Science,* **269,** 1106-1108.
NASA, G.E.S.D.a.I.S.C. (2009) Interactive Online Visualization ANd aNalysis Infrastructure (Giovanni).
Ozgul, A., Oli, M.K., Armitage, K.B., Blumstein, D.T. & Van Vuren, D.H. (2009) Influence of local demography on asymptotic and transient dynamics of a yellow-bellied marmot metapopulation. *American Naturalist,* **173,** 517-530.
Packer, C., Hilborn, R., Mosser, A., Kissui, B., Borner, M., Hopcraft, G., Wilmshurst, J., Mduma, S. & Sinclair, A.R.E. (2005) Ecological change, group territoriality, and population dynamics in Serengeti lions. *Science,* **307,** 390-393.
R, D.C.T. (2011) R: a language and environment for statistical computing. R Foundation for Statistical Computing, Vienna, Austria.
Ricker, W.E. (1954) Stock and recruitment. *Journal of the Fisheries Research Board of Canada,* **11,** 559–623.
Russell, A.F., Clutton-Brock, T.H., Brotherton, P.N.M., Sharpe, L.L., McIlrath, G.M., Dalerum, F.D., Cameron, E.Z. & Barnard, J.A. (2002) Factors affecting pup growth and survival in co-operatively breeding meerkats Suricata suricatta. *Journal of Animal Ecology,* **71,** 700-709.
Russell, A.F., Young, A.J., Spong, G., Jordan, N.R. & Clutton-Brock, T.H. (2007) Helpers increase the reproductive potential of offspring in cooperative meerkats. *Proceedings of the Royal Society of London Series B-Biological Sciences,* **274,** 513-520.
Sharp, S.P. & Clutton-Brock, T.H. (2010) Reproductive senescence in a cooperatively breeding mammal. *Journal of Animal Ecology,* **79,** 176-183.
Somers, M.J., Graf, J.A., Szykman, M., Slotow, R. & Gusset, M. (2008) Dynamics of a small re-introduced population of wild dogs over 25 years: Allee effects and the implications of sociality for endangered species' recovery. *Oecologia,* **158,** 239-247.
Stephens, P.A., Russell, A.F., Young, A.J., Sutherland, W.J. & Clutton-Brock, T.H. (2005) Dispersal, eviction, and conflict in meerkats (*Suricata suricatta*): An evolutionarily stable strategy model. *American Naturalist,* **165,** 120-135.
Stephens, P.A., Sutherland, W.J. & Freckleton, R.P. (1999) What is the Allee effect? *Oikos,* **87,** 185-190.
VanderWaal, K.L., Mosser, A. & Packer, C. (2009) Optimal group size, dispersal decisions and postdispersal relationships in female African lions. *Animal Behaviour,* **77,** 949-954.
Woodroffe, R. (2011) Demography of a recovering African wild dog (Lycaon pictus) population. *Journal of Mammalogy,* **92,** 305-315.
Worton, B.J. (1989) Kernel methods for estimating the utilization distribution in home-range studies. *Ecology,* **70,** 164-168.

Young, A.J., Carlson, A.A., Monfort, S.L., Russell, A.F., Bennett, N.C. & Clutton-Brock, T. (2006) Stress and the suppression of subordinate reproduction in cooperatively breeding meerkats. *Proceedings of the National Academy of Sciences,* **103,** 12005.

Young, A.J. & Clutton-Brock, T. (2006) Infanticide by subordinates influences reproductive sharing in cooperatively breeding meerkats. *Biology Letters,* **2,** 385-387.

Young, A.J., Spong, G. & Clutton-Brock, T. (2007) Subordinate male meerkats prospect for extra-group paternity: alternative reproductive tactics in a cooperative mammal. *Proceedings of the Royal Society B: Biological Sciences,* **274,** 1603-1609.

Table 1: results of model fitting for phenomenological group dynamics models, with most parsimonious ("best") models shown in bold

model	predictors for λ_0, K	df	$-\ln(\mathcal{L})$	ΔAIC	model weight (w)
Ricker	–	3	350.5	13.5	0.001
	D_t	5	347.6	11.8	0.002
	R_t	5	349.9	16.5	0.000
	R_t, R_{t-1}	**7**	**339.7**	**0**	**0.601**
	D_t, R_t	7	346.2	13.0	0.001
	D_t, R_t, R_{t-1}	9	339.5	3.6	0.099
Beverton-Holt	–	3	350.1	12.7	0.001
	D_t	5	348.0	12.5	0.001
	R_t	5	349.6	15.8	0.000
	R_t, R_{t-1}	**7**	**340.5**	**1.7**	**0.258**
	D_t, R_t	7	346.7	14.0	0.001
	D_t, R_t, R_{t-1}	9	340.5	5.7	0.035

Table 2: results of model fitting for component demographic rates, with maximum parsimony models used in further analyses shown in bold

demographic rate	model predictors	df	$-\ln(\mathcal{L})$	ΔAIC	model weight (w)
recruitment	N_t	3	301.3	5.7	0.022
	N_t , R_{t-1}	4	301.3	7.5	0.009
	N_t , R_t	**4**	**297.5**	**0**	**0.381**
	N_t , R_{t-1}, $N_t \cdot R_{t-1}$	5	300.1	7.2	0.011
	N_t , R_t, $N_t \cdot R_t$	5	297.4	1.8	0.153
	N_t , R_{t-1}, R_t	5	297.5	2.0	0.143
	N_t , R_{t-1}, R_t, $N_t \cdot R_{t-1}$	6	296.3	1.7	0.164
	N_t , R_{t-1}, R_t, $N_t \cdot R_t$	6	297.4	3.8	0.057
	N_t , R_{t-1}, R_t, $N_t \cdot R_{t-1}$, $N_t \cdot R_t$	7	296.3	3.7	0.061
immigration	**N_t**	**3**	**141.7**	**0**	**0.252**
	N_t , R_{t-1}	4	141.4	1.5	0.116
	N_t , R_t	4	141.5	1.7	0.110
	N_t , R_{t-1}, $N_t \cdot R_{t-1}$	5	141.4	3.5	0.043
	N_t , R_t, $N_t \cdot R_t$	5	141.4	3.5	0.043
	N_t , R_{t-1}, R_t	5	141.4	3.4	0.045
	N_t , R_{t-1}, R_t, $N_t \cdot R_{t-1}$	6	141.4	5.4	0.017
	N_t , R_{t-1}, R_t, $N_t \cdot R_t$	6	141.3	5.3	0.018
	N_t , R_{t-1}, R_t, $N_t \cdot R_{t-1}$, $N_t \cdot R_t$	7	141.2	7.2	0.007
mortality	N_t	2	281.1	21.0	<0.001
	N_t , R_{t-1}	3	280.0	20.8	<0.001
	N_t , R_t	3	278.1	17.0	<0.001
	N_t , R_{t-1}, $N_t \cdot R_{t-1}$	4	271.9	6.6	0.032
	N_t , R_t, $N_t \cdot R_t$	4	277.0	16.8	<0.001
	N_t , R_{t-1}, R_t	4	277.4	17.6	<0.001
	N_t , R_{t-1}, R_t, $N_t \cdot R_{t-1}$	5	269.8	4.4	0.094
	N_t , R_{t-1}, R_t, $N_t \cdot R_t$	5	276.1	17.1	<0.001
	N_t , R_{t-1}, R_t, $N_t \cdot R_{t-1}$, $N_t \cdot R_t$	**6**	**266.6**	**0**	**0.873**
emigration	N_t	2	376.5	52.5	<0.001
	N_t , R_{t-1}	3	349.9	1.3	0.138
	N_t , R_t	3	374.2	49.9	0.000
	N_t , R_{t-1}, $N_t \cdot R_{t-1}$	**4**	**348.3**	**0**	**0.267**
	N_t , R_t, $N_t \cdot R_t$	4	373.5	50.5	<0.001
	N_t , R_{t-1}, R_t	4	349.1	1.6	0.117
	N_t , R_{t-1}, R_t, $N_t \cdot R_{t-1}$	5	347.4	0.4	0.222
	N_t , R_{t-1}, R_t, $N_t \cdot R_t$	5	348.0	1.5	0.123
	N_t , R_{t-1}, R_t, $N_t \cdot R_{t-1}$, $N_t \cdot R_t$	6	347.0	1.4	0.132

Table 3: explanatory power of group dynamics models and contributions from model components.

model	model form [†]	R^2 [‡]	ΔR^2	% of explanatory power attributed to model component
Ricker	maximum parsimony model	0.39	–	–
	(R_{t-1})	0.20	0.19	49
	(R_t)	0.37	0.02	6
	λ_t density-independent	0.29	0.10	27
Beverton-Holt	maximum parsimony model	0.38	–	–
	(R_{t-1})	0.20	0.18	47
	(R_t)	0.35	0.02	7
	λ_t density-independent	0.29	0.08	22
combined demographic	maximum parsimony model	0.32	–	–
	(all R_{t-1} terms)	0.19	0.13	43
	(" in recruitment)	N/A	–	–
	(" in immigration)	N/A	–	–
	(" in mortality)	0.31	0.01	5
	(" in emigration)	0.22	0.10	32
	(all R_t terms)	0.32	0.01	2
	(" in recruitment)	0.32	0.01	2
	(" in immigration)	N/A	–	–
	(" in mortality)	0.33	-0.01	-4
	(" in emigration)	N/A	–	–
	(all N_t terms)	0.17	0.15	47
	(" in recruitment)	0.29	0.04	12
	(" in immigration)	0.32	0.00	0
	(" in mortality)	0.29	0.03	10
	(" in emigration)	0.28	0.05	15
	recruitment set to mean value	0.27	0.05	17
	immigration set to mean value	0.32	0.00	0
	mortality set to mean value	0.30	0.03	8
	emigration set to mean value	0.20	0.12	38

[†]Parentheses indicate omission of specified term(s) from the associated maximum parsimony model to assess explanatory power.

[‡]R^2 values were calculated based on expected and observed group sizes, assuming a null model with constant λ_t (a random walk model).

Figure 1: Phenomenological group-dynamics model predictions and observed group sizes (circles), after years of higher-than-median rainfall (black) and lower-than-median rainfall (grey), for meerkats on and near the Kuruman River Reserve, South Africa, between 1998 and 2008. Ricker (solid lines) and Beverton-Holt (dashed lines) models use group size in a given year (N_t) to predict group size in the next year (N_{t+1}). Curves show average model predictions, weighted by the number of observations in appropriate years. Dotted 1:1 line represents no year-on-year change.

Figure 2: Allee-Ricker models relating group size in a given year (N_t) to group size in the next year (N_{t+1}) for meerkats. The black curve shows the best-fit model (with no apparent Allee effect due to an Allee parameter estimate of zero); the grey curve shows the model refit with its Allee parameter fixed at 4.3 (on the edge of the 95% confidence interval as estimated for the best-fit model). Curves present average model predictions, weighted by the number of observations in each year. Dotted 1:1 line represents no year-on-year change. Rug shows observations of initial group size (plus a small amount of random noise to illustrate distribution).

Figure 3: Annual per-capita demographic rates across the observed range of initial group sizes (N_t) for meerkat groups on and near the Kuruman River Reserve, South Africa, between 1998 and 2008. Curves show average model predictions, weighted by the number of observations in appropriate years. Circles show corresponding observations. **A**: recruitment rate (recruits/N_t; note different scale) *in* years of higher-than-median (black) and lower-than-median (grey) annual rainfall; **B**: immigration rate (immigrants/N_t); **C**: mortality rate (deaths/[N_t + recruits + immigrants]) *after* years of higher-than-median (black) and lower-than-median (grey) annual rainfall; **D**: emigration rate (emigrants/[N_t + recruits + immigrants]) *after* years of higher-than-median (black) and lower-than-median (grey) annual rainfall.

Figure 4: Predictions from "combined demographic" group-dynamics model (solid lines) and observed group sizes (circles), after years of higher-than-median rainfall (black) and lower-than-median rainfall (grey), for meerkats on and near the Kuruman River Reserve, South Africa, between 1998 and 2008. The model combines sub-models of component demographic rates to predict change between group size in a given year (N_t) and group size in the next year (N_{t+1}). Curves show average model predictions, weighted by the number of observations in appropriate years. Dotted 1:1 line represents no year-on-year change.

Figure 5: Annual per-capita changes in group size (λ_t) for meerkats on and near the Kuruman River Reserve, South Africa, for years 2000 (grey) and 2006 (black). Circles

show observations and solid lines show predictions from a model combining sub-models for component demographic rates to predict change between group size in a given year (N_t) and group size in the next year. Dotted line represents no year-on-year change.

Figure 1:

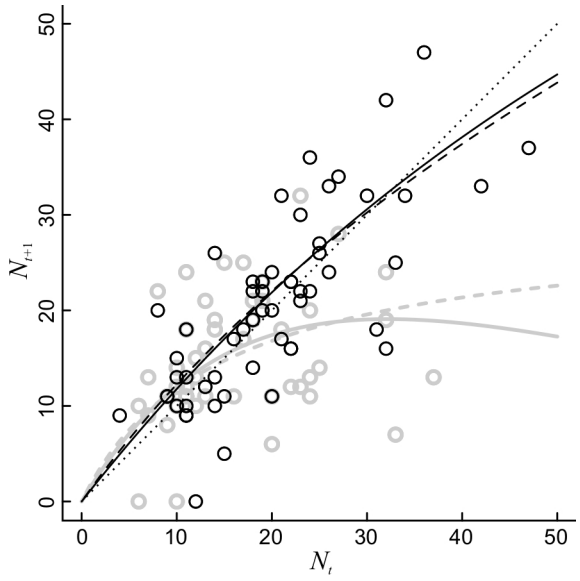

Figure 2:

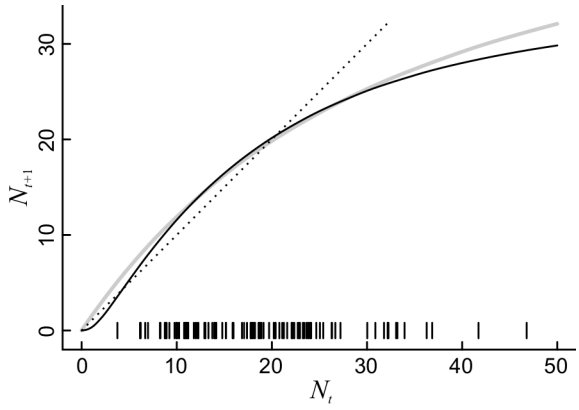

Figure 3:

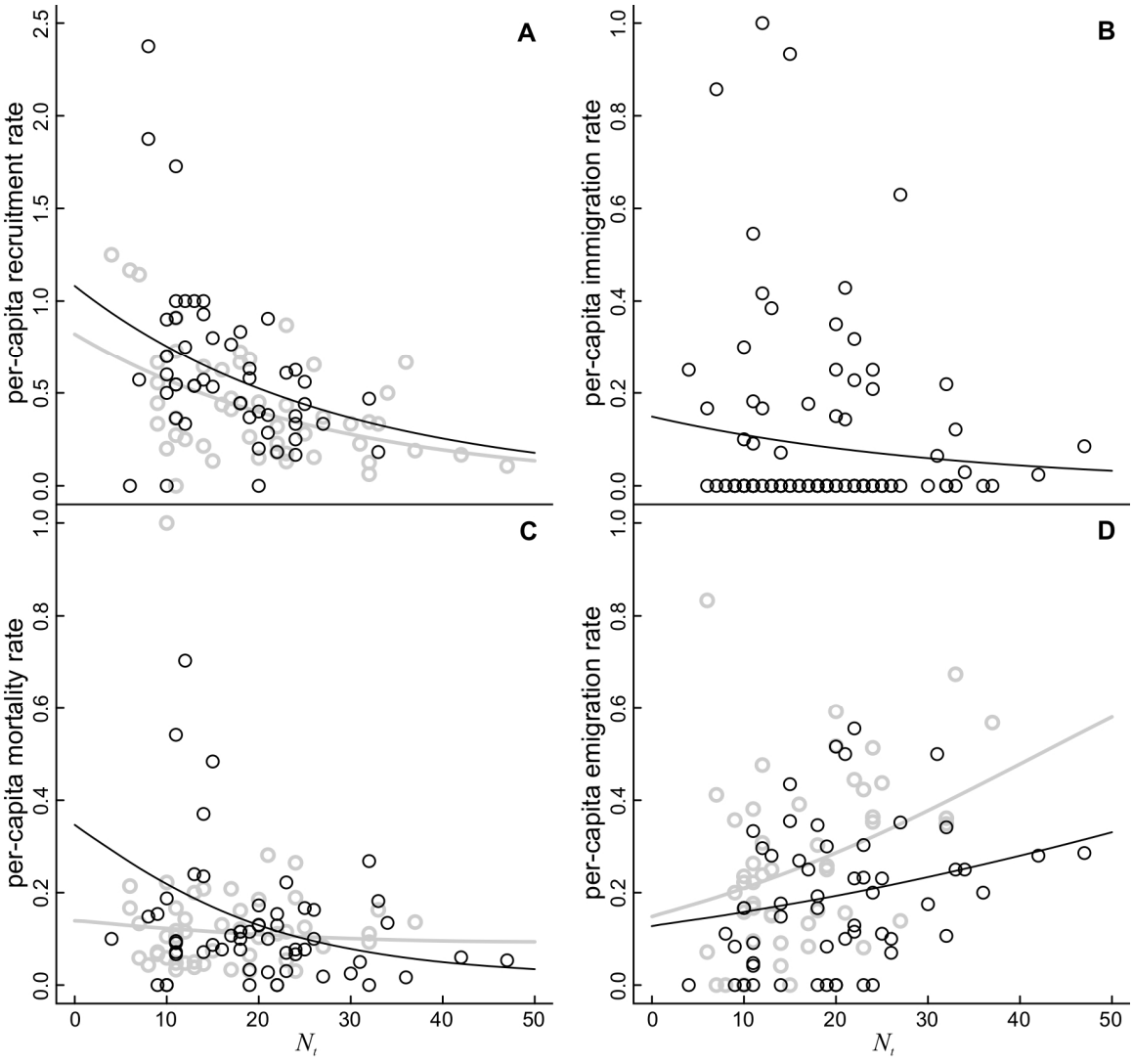
A
B
C
D
per-capita recruitment rate
per-capita immigration rate
per-capita mortality rate
per-capita emigration rate
N_t
N_t

Figure 4:

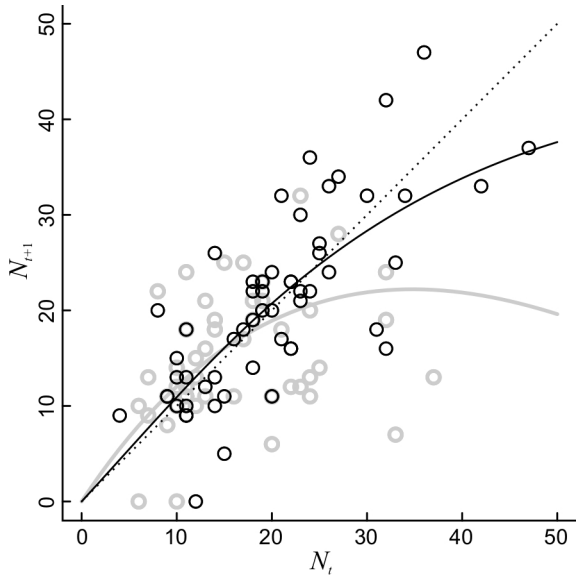

Figure 5: